Journal of Experimental Botany, Vol. 57, No. 14, pp. 3883–3900, 2006
doi:10.1093/jxb/erl156 Advance Access publication 17 October, 2006

Journal of Experimental Botany

RESEARCH PAPER

Determining RuBisCO activation kinetics and other rate and equilibrium constants by simultaneous multiple non-linear regression of a kinetic model

Dennis McNevin[1], Susanne von Caemmerer[1,*] and Graham Farquhar[2]

[1] *Molecular Plant Physiology Group, Research School of Biological Sciences, Building 46, The Australian National University, Canberra, ACT 0200, Australia*

[2] *Environmental Biology Group, Research School of Biological Sciences, The Australian National University, Canberra, ACT 0200, Australia*

Received 28 May 2006; Accepted 10 August 2006

Abstract

The forward and reverse rate constants involved in carbamylation, activation, carboxylation, and inhibition of D-ribulose-1,5-*bis*phosphate carboxylase/oxygenase (RuBisCO) have been estimated by a new technique of simultaneous non-linear regression of a differential equation kinetic model to multiple experimental data. Parameters predicted by the model fitted to data from purified spinach enzyme *in vitro* included binding affinity constants for non-substrate CO_2 and Mg^{2+} of 200±80 μM and 700±200 μM, respectively, as well as a turnover number (k_{cat}) of 3.3±0.5 s^{-1}, a Michaelis half-saturation constant for carboxylation ($K_{M,C}$) of 10±4 μM and a Michaelis constant for RuBP binding ($K_{M,RuBP}$) of 1.5±0.5 μM. These and other constants agree well with previously measured values where they exist. The model is then used to show that slow inactivation of RuBisCO (fallover) in oxygen-free conditions at low concentrations of CO_2 and Mg^{2+} is due to decarbamylation and binding of RuBP to uncarbamylated enzyme. In spite of RuBP binding more tightly to uncarbamylated enzyme than to the activated form, RuBisCO is activated at high concentrations of CO_2 and Mg^{2+}. This apparent paradox is resolved by considering activation kinetics and the fact that while RuBP binds tightly but slowly to uncarbamylated enzyme, it binds fast and loosely to activated enzyme. This modelling technique is presented as a new method for determining multiple kinetic data simultaneously from a limited experimental data set. The method can be used to compare the properties of RuBisCO from different species quickly and easily.

Key words: Activation, binding, carbamylation, enzyme, equilibrium constant, fallover, kinetic, rate constant, RuBisCO, simulation.

Introduction

D-ribulose-1,5-*bis*phosphate carboxylase/oxygenase (RuBisCO, EC 4.1.1.39) catalyses the carboxylation and oxygenation of D-ribulose-1,5-*bis*phosphate (ribulose-P_2 or RuBP) in photosynthetic CO_2 fixation and photorespiration. The reaction proceeds by way of a two-step process. The first step involves carbamylation of an uncharged amino group at Lysine-201 (of the spinach sequence) by non-substrate CO_2 and subsequent coordination of Mg^{2+} to one of the carbonyl oxygens of the carbamate resulting in an activated enzyme (Laing and Christeller, 1976; Lorimer *et al*., 1976; Andrews, 1996). The second step occurs as substrate RuBP is bound in the vicinity of the carbamate and then combined with either CO_2 (carboxylation) to form two molecules of 3-phosphoglycerate (PGA) or with O_2 (oxygenation) to form one molecule each of PGA and 2-phosphoglycolate (2PG). (Laing and Christeller, 1976; Badger and Collatz, 1977; Andrews and Lorimer, 1987).

RuBisCO is the most abundant protein on earth, representing some 30–50% of the soluble protein in the

* To whom correspondence should be addressed. E-mail: susanne.caemmerer@anu.edu.au

Abbreviations: 2PG, 2-phosphoglycolate; CA1P, 2-carboxy-arabinitol-1-phosphate; CABP, 2-carboxy-arabinitol-1,5-*bis*phosphate; PDBP, D-*glycero*-2, 3-pentodiulose-1,5-*bis*phosphate; PGA, 3-phosphoglycerate; RuBisCO, D-ribulose-1,5-*bis*phosphate carboxylase/oxygenase; RuBP, D-ribulose-1, 5-*bis*phosphate; XuBP, D-xylulose-1,5-*bis*phosphate.

leaves of C_3 plants and has been the subject of much interest as a means of understanding and improving agricultural crop and green biomass productivities. Recently, attention has turned to the possibility of replacing native RuBisCO in agriculturally important plants with that from another species where the introduced protein displays superior carboxylation kinetics under physiological conditions (see Andrews and Whitney, 2003; Parry *et al*., 2003, for recent reviews as well as Tcherkez *et al*., 2006). The ability to screen suitable candidates for transgenic manipulation has become very important. Historically, estimates of the turnover number for carboxylation (k_{cat}), the Michaelis–Menten (half-saturation) coefficient for carboxylation (with respect to CO_2), $K_{M,C}$, and the specificity for carboxylation over oxygenation, $S_{C/O}$, have served as indicators of performance. However, these numbers will only discriminate between enzymes if all other factors are equal. For example, little account has been taken of the carbamylation/activation state of the enzyme under differing physiological conditions; of the Michaelis–Menten coefficient with respect to RuBP ($K_{M,RuBP}$); and of the relative binding affinities of RuBP for active and inactive enzyme.

Binding of sugar bisphosphates (other than RuBP to activated enzyme) detracts from RuBisCO's carboxylation potential. Sugar phosphates can bind to carbamylated and uncarbamylated RuBisCO active sites. In general, positive effectors bind more tightly to the activated form of RuBisCO and stabilize the active state, whereas negative effectors bind more tightly to the unactivated form and prevent activation (Hatch and Jensen, 1980; Badger and Lorimer, 1981; Jordan *et al*., 1983). Positive effectors compete in the carboxylase reaction with RuBP and act as competitive inhibitors (Laing and Christeller, 1976; Badger and Lorimer, 1981; Frank *et al*., 1998). They are generally alternative bisphosphates which mimic RuBP or its enediolized form and eventually lead *in vitro* to the slow, first-order decline in RuBisCO activity to a final steady state (the so-called 'fallover' phenomenon) (Andrews and Lorimer, 1987; Pearce and Andrews, 2003). RuBP can also bind to unactivated RuBisCO. Laing and Christeller (1976) and Jordan and Chollet (1983) proposed that fallover occurs because of binding of the substrate to the unactive enzyme following decarbamylation, although this has been challenged by Edmondson *et al*. (1990*a*, *b*, *c*) who showed that decarbamylation did not occur during fallover in their experiments and proposed that catalytic misfiring produces an inhibitor which binds to the active site. Nevertheless, RuBP binds more tightly to the unactivated enzyme than to the activated enzyme (Laing and Christeller, 1976; Vater and Salnikow, 1979) resulting in 'dead-end' inhibition (Andrews, 1996; Spreitzer and Salvucci, 2002).

Even RuBP bound to activated RuBisCO can undergo epimerization at the active site to form inhibitory compounds. Most notable of these are D-xylulose-1,5-*bis*phosphate (xylulose-P_2 or XuBP), which arises from misprotonation of the enediolate during carboxylation (Zhu and Jensen, 1991; Edmondson *et al*., 1990*d*), and D-*glycero*-2,3-pentodiulose-1,5-*bis*phosphate (PDBP), which is a result of H_2O_2 elimination from the peroxyketone intermediate during oxygenation (Chen and Hartman, 1995; Kim and Portis, 2004). Zhu and Jensen (1991) showed that inhibition of activated RuBisCO by XuBP is a slow process (20–30 min) and is consistent with a mechanism where XuBP binds more tightly to uncarbamylated RuBisCO than to carbamylated RuBisCO. The slow kinetics reflected the requirement for decarbamylation to occur before tight binding of the inhibitor.

Pearce and Andrews (2003) have proposed that 'fallover' inhibition may have developed in higher plants as a consequence of higher CO_2 specificity characterized by greater affinity for the carboxylated (rather than oxygenated) intermediate and subsequent misprotonation. This effect has been mitigated by the evolution of RuBisCO activase which rapidly releases all sugar bisphosphates from the active site, including RuBP, XuBP, and 2-carboxy-arabinitol-1-phosphate (CA1P), a tight binding inhibitor which is bound to RuBisCO in many plant species at night (Parry *et al*., 2003), perhaps protecting RuBisCO from degradation by proteases. The advent of activase has resulted in a sophisticated regulatory system for RuBisCO activity (Portis, 2003).

While the overall reaction mechanism for RuBisCO has been well characterized and some equilibrium relationships determined, the kinetic rates for these steps are much less understood. The rates and equilibrium constants associated with ligand binding are difficult to measure with existing experimental methods. Dynamic modelling of more than a few rates simultaneously has required computing power which has only recently become available. A computer-based method of simultaneous, non-linear regression of a differential equation model to experimental time series (transients) is presented as an efficient and powerful way to determine catalytic rate constants, greatly minimizing the amount of experimental data required to parameterize kinetic models. The advantages of non-linear regression over linear regression for enzyme kinetic data and associated error distributions have been previously documented (Leatherbarrow, 1990). The result is a holistic kinetic model of RuBisCO with many kinetic parameters fitted to experimental data in oxygen-free conditions. In particular, the activation kinetics of RuBisCO, as well as the carboxylation kinetics, are quantified. It has also been possible to gain some insights into the 'fallover' phenomenon as a result of model simulations and thus light has been shed on a subject which has been the subject of much previous speculation (Jordan and Chollet, 1983; Edmondson *et al*., 1990*a*, *b*, *c*, *d*). The model represents a new comparative tool to produce kinetic data for RuBisCO from a range of species and, indeed, for enzymes in general. Models such as that presented here represent a new type of *in silico* experimental system (Peck,

2004; McCulloch and Huber, 2002) and are a powerful way to examine complex systems whose behaviours would otherwise be difficult to predict.

Materials and methods

Materials

RuBisCO was purified from the leaves of spinach (*Spinacea oleracea*) plants using a procedure involving polyethylene glycol precipitation followed by anion-exchange chromatography (ÄKTA™ explorer, Amersham Pharmacia Biotech, Uppsala) on a Waters (Milford, MA) Protein-Pak™ Q column, essentially as described by Edmondson *et al*. (1990*a*), but omitting the final gel filtration step (Morell *et al*., 1997), which in turn is based on an original method by Hall and Tolbert (1978). RuBP was prepared enzymatically from D-ribose-5-phosphate according to the procedure of Edmondson *et al*. (1990*a*) based on the method of Horecker *et al*. (1958). The production of PGA as a result of carboxylation of RuBP by RuBisCO served as an indicator of the progress of reaction in a modification of a spectrophotometric assay (Lilley and Walker, 1974). PGA formation in solution was enzymatically coupled to NADH oxidation as described by Pearce and Andrews (2003). The change in concentration of NADH (and hence, PGA formation) was monitored by absorbance at 340 nm on a diode array spectrophotometer (Hewlett Packard, 8452A). The initial concentration of NADH (200 μM) was always in excess of that which would be oxidized if all RuBP was converted to PGA.

Experimental approach

A set of 18 experimental time-courses or transients were produced in 18×2 ml total reaction volumes which were each subjected to nitrogen sparging until they were covered with a 1 ml layer of paraffin oil. This prevented the ingress or egress of O_2 and CO_2. They were each buffered at pH 8.0 with final concentrations of 80 mM EPPS and 1 mM EDTA which had been previously sparged overnight with nitrogen gas to remove O_2 and CO_2 and each contained 0.1 mg ml^{-1} carbonic anhydrase. The solutions varied as to whether they subsequently contained 2.5 mM, 5 mM or 10 mM $NaHCO_3$ and 2 mM, 5 mM or 25 mM $MgCl_2$, making 3×3=9 concentration combinations. They were incubated for 30 min at 25 °C but also varied as to whether this was in the presence or in the absence of 3 μg ml^{-1} RuBisCO isolated from spinach (equivalent to approximately 30–40 nM active sites). In the former case, RuBisCO was deemed to be 'activated' while in the latter case, where RuBisCO was added later with RuBP, the results were deemed to be those of 'unactivated' RuBisCO. This made a total of 2×9=18 different experimental conditions. After incubation for 30 min, RuBP was added to a concentration of 40 μM (simultaneously with 3 μg ml^{-1} RuBisCO for those reactions where RuBisCO was not already present) in order to initiate carboxylation. In each case, the progress of reaction (production of PGA) was monitored via spectrophotometric assay for a further 30 min with stirring.

This procedure was repeated twice more to produce additional experimental data where the concentrations of reactants were varied. In the first repeat, the concentrations of $NaHCO_3$ were changed to 2 mM, 4 mM, and 6 mM and the concentrations of $MgCl_2$ were changed to 15 mM, 20 mM, and 25 mM. In the second repeat, the concentration of $MgCl_2$ was held constant at 25 mM, but the concentrations of RuBP added to initiate carboxylation were 10 μM, 20 μM, and 40 μM. The repeats resulted in a total data set of 3×18 experimental transients. The RuBisCO model described below was independently fitted to these three data sets so as to estimate errors in fitted parameters.

Mathematical model of RuBisCO

A mathematical model of RuBisCO activity was developed according to Fig. 1, reflecting current understanding of the RuBisCO reaction mechanism. In this paper, RuBisCO activity *in vitro* in oxygen-free conditions is considered and thus oxygenation is neglected in our model. Note that binding of sugar bisphosphates (RuBP and XuBP) to carbamylated (but not fully activated) enzyme has been included. This binding has been speculated about elsewhere (Laing and Christeller, 1976; Badger and Lorimer, 1981; Edmondson *et al*., 1990*b*) and there is no known reason why it should not occur. In fact, our model provided a better 'fit' of rate constants to experimental data when this binding was included. The model describes the rates of accumulation and depletion of the following species in oxygen-free solution: E, ER, EX, EC, ECR, ECX, ECM, ECMR, ECMX,

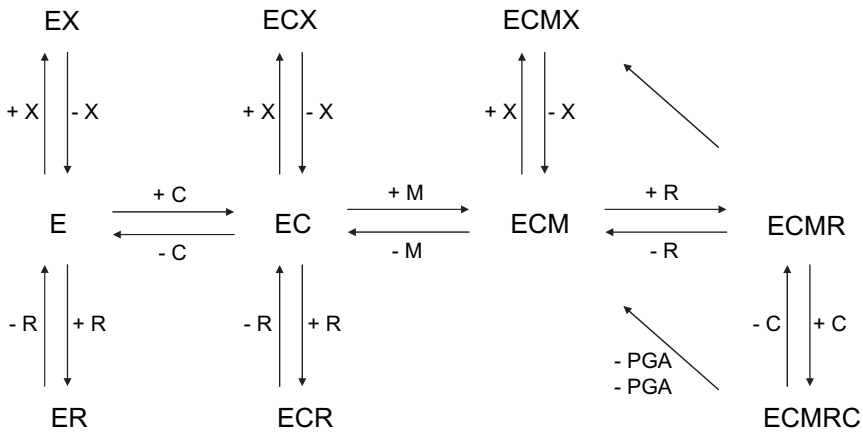

Fig. 1. Model of RuBisCO reaction mechanism in an oxygen-free environment (oxygenation neglected). Double arrows represent reversible reactions while single arrows represent irreversible reactions. Free enzyme (E) is carbamylated with CO_2 (C) to form carbamylated enzyme (EC) which in turn co-ordinates with Mg^{2+} (M) to form the activated enzyme (ECM). RuBP (R) binds to activated enzyme to form an enzyme–substrate complex (ECMR) which undergoes carboxylation to form the reaction intermediate (ECMRC) and this decomposes back to the activated enzyme, releasing the reaction products, two molecules of PGA, in the process. The enzyme substrate complex can undergo misprotonation such that XuBP (X) is produced at the active site (ECMX). XuBP and RuBP can also bind to free enzyme and carbamylated enzyme to form the complexes EX, ECX, ER, and ECR.

ECMRC, C, R, M, X, PGA (see Fig. 1 for explanation of symbols). Each species is subject to accumulation and depletion determined by forward and reverse rates, where forward rates describe the rate of association of enzyme–ligand complexes and reverse rates describe the rate of dissociation of enzyme–ligand complexes. For example, consider the free (uncarbamylated) enzyme, E (Fig. 1), with concentration [E] (mol l^{-1} or M). A mass balance yields:

$$\frac{d[E]}{dt} = \upsilon_{r,EC} - \upsilon_{f,EC} + \upsilon_{r,ER} - \upsilon_{f,ER} + \upsilon_{r,EX} - \upsilon_{f,EX}$$

where υ (M s^{-1}) are molar rates and the subscripts f and r refer to forward and reverse, respectively. Hence, $\upsilon_{f,EC}$ is the (forward) rate of association of the enzyme–ligand complex EC from its components, E and C, while $\upsilon_{r,EC}$ is the (reverse) rate of dissociation of EC into its components, E and C. A similar mass balance is performed for each species. Now, each of the molar rates can be described by elementary kinetic expressions as, for example:

$$\upsilon_{f,EC} = k_{f,EC}[E][C]$$

$$\upsilon_{r,EC} = k_{r,EC}[EC]$$

where $k_{f,EC}$ ($M^{-1}s^{-1}$) and $k_{r,EC}$ (s^{-1}) are the forward and reverse rate constants, respectively. These are the 'unknowns' which are 'fitted' to experimental data. For each enzyme–ligand complex, the forward and reverse rate constants define an equilibrium constant as, for example:

$$\frac{k_{r,EC}}{k_{f,EC}} = K_{EC}$$

where K_{EC} is the (equilibrium) binding affinity constant for the enzyme–ligand complex, EC. It is then only at steady-state that:

$$K_{EC} = \frac{[E]_{eq}[C]_{eq}}{[EC]_{eq}}$$

where the subscript 'eq' refers to equilibrium concentrations. There are two special conditions for which it is assumed that the rates are irreversible or negligibly reversible. These are the product forming reaction (ECMRC→ECM+2 PGA) and the misprotonation reaction (ECMR→ECMX) described by:

$$\upsilon_{cat} = k_{cat}[ECMRC]$$

and

$$\upsilon_{mis} = k_{mis}[ECMR]$$

where the subscripts 'cat' and 'mis' refer to the intrinsic catalytic rate for PGA formation and the enediolate misprotonation rate, respectively. Note that k_{cat} (s^{-1}) is the catalytic turnover number for carboxylation and k_{mis} (s^{-1}) is the catalytic turnover number for misprotonation. There is no equilibrium expression for these irreversible rates. They are equivalent to reverse rates (and have the same units) in that they describe the dissociation (or rearrangement) of an enzyme–ligand complex.

The complete set of 17 differential mass balances and 20 unknown rate constants describing the system depicted in Fig. 1 is included in the Appendix. They account for the ten enzyme species (E, ER, EX, EC, ECR, ECX, ECM, ECMR, ECMX, ECMRC), the carbamylation and carboxylation substrate CO_2 (C), two sugar bisphosphates (R, X), the sugar phosphate reaction product of carboxylation (PGA), and Mg^{2+} (M).

Numerical model of RuBisCO

The 17 differential mass balances described in the Appendix were coded into a MATLAB (MathWorks, 2002) function (m file) which returns the vector d**y**/dt given by:

$$\frac{d\mathbf{y}}{dt} = f(\mathbf{y}, \mathbf{k})$$

where **y** is an input vector of the17 variable values and **k** is an input vector of the 20 unknown rate constants. This function was then used as input to an ordinary differential equation (ODE) solver (MATLAB function ode15s) using Gear's method of backward differentiation for a system of ODEs (Shampine and Reichelt, 1997). For a nominated time period and a set of initial variable conditions, $\mathbf{y}_0$, the solver returns the vector **y** given by:

$$\mathbf{y} = f(t, \mathbf{k})$$

which represents the solution (as a function of time) to the set of differential mass balances comprising the RuBisCO model and which can be fitted to experimental data by varying **k**.

Non-linear regression

The model-generated output returned by the ODE solver was then used as input for a non-linear least-squares curve-fitting algorithm (MATLAB function lsqcurvefit) from the MATLAB Optimization Toolbox. This algorithm is a subspace trust region method and is based on the interior-reflective Newton method (Coleman and Li, 1996). Each iteration involves the approximate solution of a large linearized system using the method of preconditioned conjugate gradients. Given 60 time points, t_j, (1 min intervals over 60 min) and the matrix of observed experimental data, $\mathbf{x}_{i,j}$, consisting of 18 experimental transients over 60 time points, this function finds the vector of coefficients, **k**, that minimizes the function:

$$\frac{1}{2}\sum_{i=1}^{18}\sum_{j=0}^{60}\left(F(\mathbf{k}, t_j) - \mathbf{x}_{i,j}\right)^2$$

where $F(\mathbf{k}, t_j)$ is the matrix of model-generated outputs at time points, t_j, for the 18 different experimental conditions. In other words, this algorithm finds the set of 20 rate constants that best fits 18 model-generated transients simultaneously to the 18 experimental transients when the model is provided with the same initial conditions and discontinuities as the experimental data.

The optimization algorithm represents a complex, non-linear and stiff (wide range of rate constant values) system of 17 differential equations and 20 rate constants fitted to 18 experimental transients. Any global minimum solution is then inevitably surrounded by multiple local minima. The curve-fitting function was therefore governed by a supervising MATLAB function that varied **k** randomly once a local minimum solution was found. Any new minimum solution was then compared with the original solution and accepted as a better solution if the sum of the residuals was less. This process was continued until no further improvement was attained and it was assumed that the global minimum had been achieved.

The model was fitted independently to each of the three sets of 18 experimental transients described earlier. For each set of 18 transients, the model was fitted five times from different initial estimates of the kinetic constants in order to determine the robustness of the solution. This resulted in 3×5=15 estimates for each of the kinetic constants from which their precision could be estimated.

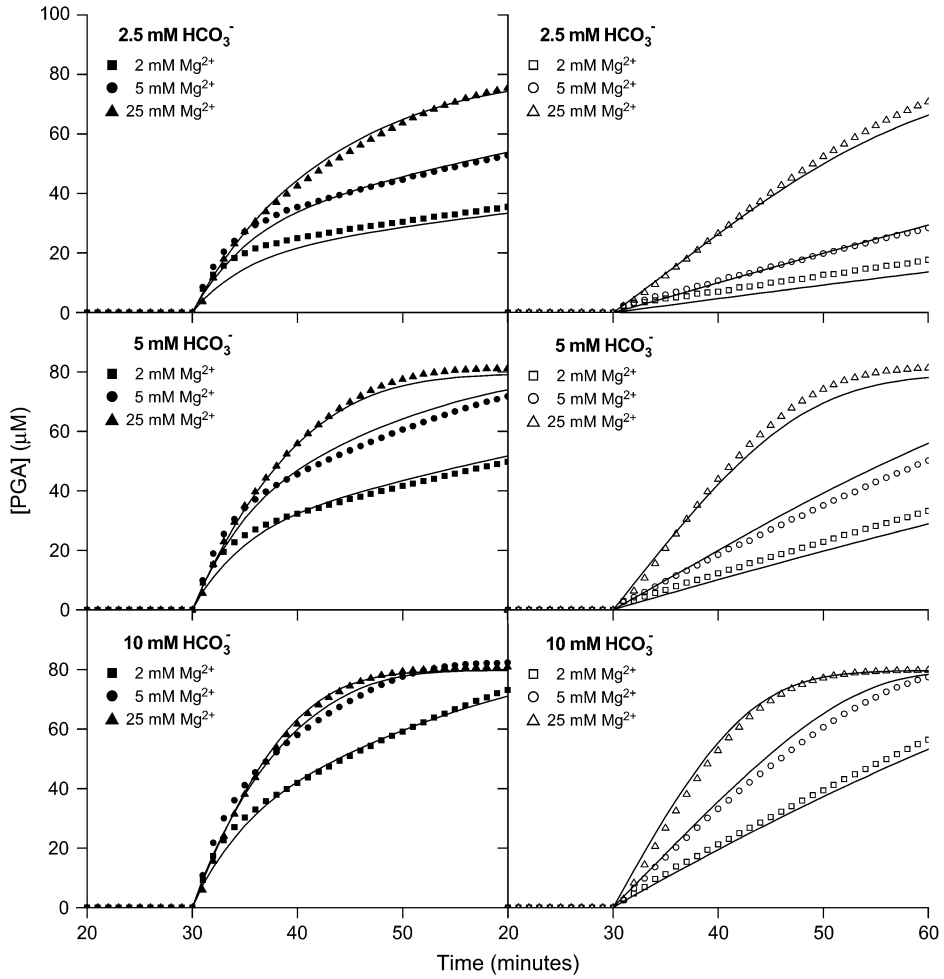

Fig. 2. Data points for a single set of 18 experimental transients at pH 8.0 and 25 °C representing PGA concentration at 1 min intervals over the course of the 60 min reaction where carboxylation was initiated at 30 min. The concentration of HCO_3^- was either 2.5 mM (top), 5 mM (middle), or 10 mM (bottom). The concentration of Mg^{2+} was either 2 mM (squares), 5 mM (circles) or 25 mM (triangles). Prior to initiation of carboxylation by addition of RuBP, RuBisCO was either activated (left: closed symbols) or unactivated (right: open symbols). Unbroken lines represent the model output under the same conditions. This particular 'fit' resulted in a sum of residuals of 3.25×10^{-9} M^2.

Results

A set of 18 experimental transients and 'best fit' model output are displayed in Fig. 2. This figure is typical of each of the five regressions to each of the three sets of 18 transients and qualitatively reflects the transients observed by Laing and Christeller (1976) under similar conditions. The model accurately predicts non-steady-state dynamics or rates (represented by 'curves' in Fig. 2) as well as pseudo-steady-state conditions or equilibria (represented by 'straight lines' in Fig. 2). The mean rate constants resulting from all 15 regressions are given in Table 1 together with derived equilibrium constants. Commonly measured Michaelis–Menten (half-saturation) constants have also been calculated. In the absence of oxygenation, the half-saturation constant for carboxylation, $K_{M,C}$, is (von Caemmerer, 2000; Farquhar, 1979):

$$K_{M,C} = \frac{k_{cat} + k_{r,ECMRC}}{k_{f,ECMRC}}$$

In the absence of oxygenation, the half-saturation constant for binding of RuBP to activated RuBisCO, $K_{M,RuBP}$, is (von Caemmerer, 2000; Farquhar, 1979):

$$K_{M,RuBP} = \frac{k_{ECMR} + \frac{k_{cat}}{k_{f,ECMR}}\frac{[C]}{K_{M,C}}}{1 + \frac{[C]}{K_{M,C}}}$$

$K_{M,RuBP}$ depends on the concentration of CO_2 and so it has been calculated at pH 8.0 for the theoretical range where [C] varies from zero to infinity (i.e. $k_{cat}/k_{f,ECMR} < K_{M,RuBP} < K_{ECMR}$). The mean values for the rate constants (averaged over values from all 15 regressions) are then included in Fig. 3, together with the mean values for the derived equilibrium constants, each with appropriate significant figures.

The simultaneous non-linear regression was tested for sensitivity to any of the fitted rate constants. Each of the constants was individually reduced and increased by its standard error (Table 1) and the sum of residuals was

Table 1. *Rate constants and derived (equilibrium) binding affinity constants (reverse rate constant divided by forward rate constant) that best fit the RuBisCO model to the three sets of 18 experimental transients at 25 °C from five different initial values (with standard errors)*

[Mg^{2+}]	Units	2, 5, 25 mM		15, 20, 25 mM		25 mM		Overall	
[HCO_3^-]		2.5, 5, 25 mM		2, 4, 6 mM		2, 4, 6 mM			
[RuBP]		40 μM		40 μM		10, 20, 40 μM			
		Mean	Error	Mean	Error	Mean	Error	**Mean**	Error
	Rate constants								
k_{cat}	s^{-1}	3.4	0.6	3.2	0.6	3.4	0.4	**3.3**	0.5
k_{mis}	s^{-1}	0.33	0.23	0.24	0.07	0.27	0.08	**0.28**	0.14
$k_{f,ECMRC}$	$mM^{-1}\ s^{-1}$	600	120	660	20	360	110	**540**	160
$k_{r,ECMRC}$	s^{-1}	2.1	0.9	1.3	0.6	1.3	1.6	**1.6**	1.1
$k_{f,ECMR}$	$mM^{-1}\ s^{-1}$	3700	100	5400	900	3900	500	**4300**	900
$k_{r,ECMR}$	s^{-1}	5.9	0.8	5.1	2.0	7.0	1.2	**6.0**	1.5
$k_{f,ECMX}$	$mM^{-1}\ s^{-1}$	2000	800	3800	900	2500	700	**2800**	1100
$k_{r,ECMX}$	s^{-1}	0.104	0.016	0.053	0.043	0.068	0.013	**0.075**	0.034
$k_{f,ECM}$	$mM^{-1}\ s^{-1}$	3.2	0.2	10.7	4.9	4.4	0.9	**6.1**	4.3
$k_{r,ECM}$	s^{-1}	2.7	0.2	5.3	1.6	3.2	0.7	**3.7**	1.5
$k_{f,ECX}$	$mM^{-1}\ s^{-1}$	3000	1800	2700	800	2800	600	**2900**	1100
$k_{r,ECX}$	s^{-1}	0.0024	0.0002	0.0051	0.0021	0.0034	0.0014	**0.0036**	0.0018
$k_{f,ECR}$	$mM^{-1}\ s^{-1}$	45	9	37	14	51	19	**44**	15
$k_{r,ECR}$	s^{-1}	0.029	0.014	0.018	0.026	0.038	0.019	**0.028**	0.020
$k_{f,EC}$	$mM^{-1}\ s^{-1}$	1.1	0.3	1.2	0.1	0.6	0.2	**1.0**	0.4
$k_{r,EC}$	s^{-1}	0.13	0.02	0.27	0.07	0.13	0.06	**0.18**	0.09
$k_{f,EX}$	$mM^{-1}\ s^{-1}$	28	5	15	8	22	3	**22**	8
$k_{r,EX}$	s^{-1}	0.0008	0.0002	0.0004	0.0003	0.0008	0.0002	**0.0007**	0.0003
$k_{f,ER}$	$mM^{-1}\ s^{-1}$	43	14	23	10	57	25	**41**	21
$k_{r,ER}$	s^{-1}	0.0019	0.0003	0.0006	0.0011	0.0028	0.0010	**0.0018**	0.0012
	Equilibrium constants								
K_{ECMRC}	μM	3.9	2.2	2.0	0.9	3.2	4.1	**2.8**	2.7
K_{ECMR}	μM	1.6	0.2	1.0	0.6	1.8	0.4	**1.5**	0.5
K_{ECMX}	μM	0.056	0.016	0.017	0.020	0.029	0.006	**0.033**	0.023
K_{ECM}	μM	840	110	610	310	710	40	**710**	210
K_{ECX}	μM	0.0010	0.0004	0.0018	0.0004	0.0012	0.0003	**0.0013**	0.0005
K_{ECR}	μM	0.6	0.2	0.4	0.4	0.7	0.2	**0.6**	0.3
K_{EC}	μM	110	10	220	40	240	110	**200**	80
K_{EX}	μM	0.027	0.003	0.028	0.002	0.038	0.008	**0.031**	0.007
K_{ER}	μM	0.047	0.008	0.015	0.025	0.053	0.021	**0.039**	0.026
$K_{M,C}$	μM	9.8	4.2	6.9	1.7	13.1	4.2	**9.7**	4.3
$K_{M,RuBP}$ ([C] → 0)	μM	1.6	0.2	1.0	0.6	1.8	0.4	**1.5**	0.5
$K_{M,RuBP}$ ([C] → ∞)	μM	0.9	0.2	0.6	0.3	0.9	0.2	**0.8**	0.2

recalculated from the resulting model simulation for each of the three sets of 18 experimental transients to determine any differences in the 'fit' that arose. The results are displayed in Fig. 4 which shows that the regression is only sensitive in all three cases to change in the forward (formation) rate constant for the complex ER ($k_{f,ER}$). It is sensitive to the reverse (decomposition) rate for this complex ($k_{r,ER}$) in only two out of three sets. Other constants to which the regression is sensitive include the forward rate constant for EC (in two sets), the reverse rate constant for EC (in one set), the reverse rate constant for ECMX (in one set), the forward and reverse rate constants for ECMRC (in one set), and the misprotonation rate constant (in one set). The regression appears to be less sensitive to changes in other parameters, indicating that they may take on a wider range of values without affecting the kinetic response of the model under the experimental conditions examined. For example, the model is relatively insensitive to the forward and reverse rate constants for the complexes EX ($k_{f,EX}$ and $k_{r,EX}$, respectively). It might be expected that rate constants associated with the formation of the carbamylated and activated enzyme (e.g. EC) as well as with enzyme bound RuBP (e.g. ER) would be accurately determined because the experimental procedure involved changes in concentrations of the ligands CO_2 (C) and RuBP (R). One would be less confident of constants associated with XuBP because the concentration of this ligand was inferred rather than directly measured.

The model predicted transients deviate most from the experimental data within the first 10 min after initiation of carboxylation at 2 mM Mg^{2+} for activated enzyme. The model was refitted to this first 10 min of data after parameters were initialized with values that best fit the complete time-course (from Table 1). The largest changes were observed for $k_{f,EC}$, $k_{f,EX}$, $k_{r,EX}$, and $k_{f,ER}$, which

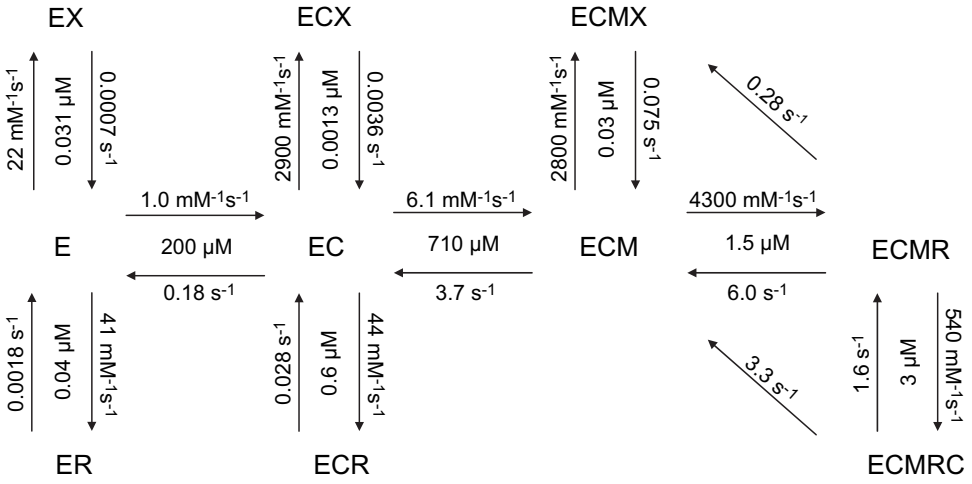

Fig. 3. Mean forward rates ($mM^{-1}\ s^{-1}$), reverse rates (s^{-1}) and derived (equilibrium) binding affinity constants (μM) that best fit the RuBisCO model to the 3×18 experimental transients at pH 8.0 and 25 °C.

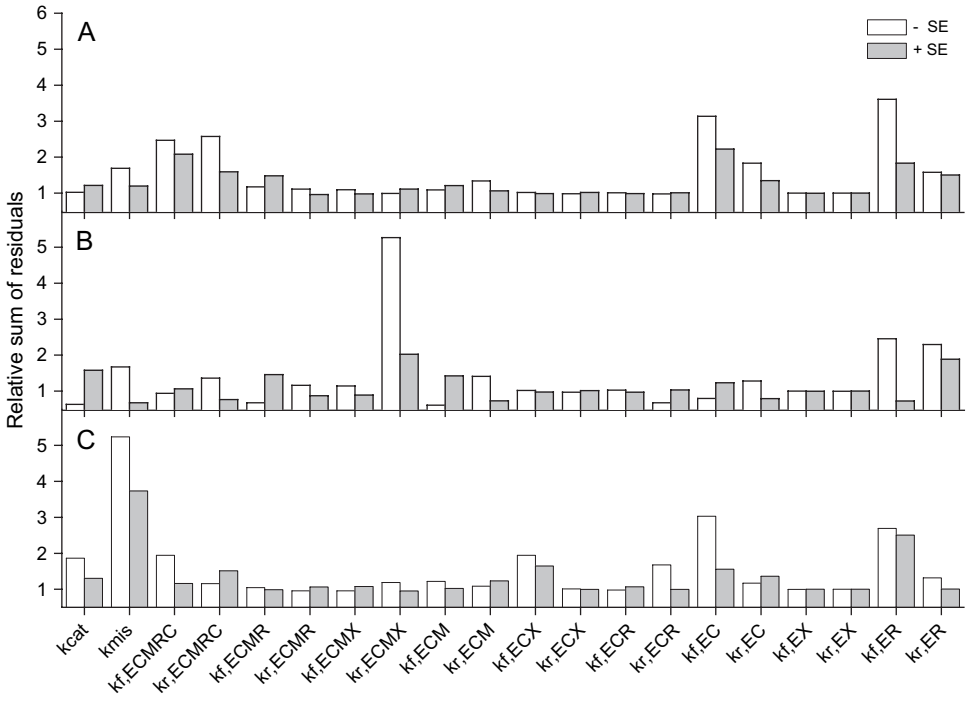

Fig. 4. Sensitivity (in terms of the relative change in the sum of residuals) of the simultaneous non-linear regression to changes in the fitted rate constants for each of the three sets of 18 experimental transients. The mean values of the constants were each individually reduced by their standard error (–SE) and increased by their standard error (+SE). Each of the three sets of transients differed as to the concentrations of Mg^{2+}, HCO_3^- and RuBP in three ways as follows: (A) $[Mg^{2+}]$=2 mM, 5 mM, 25 mM; $[HCO_3^-]$=2.5 mM, 5 mM, 10 mM; [RuBP]=40 μM; (B) $[Mg^{2+}]$=15 mM, 20 mM, 25 mM; $[HCO_3^-]$=2 mM, 4 mM, 6 mM; [RuBP]=40 μM; (C) $[Mg^{2+}]$=25 mM; $[HCO_3^-]$=2 mM, 4 mM, 6 mM; [RuBP]=10 μM, 20 μM, 40 μM.

increased approximately 2-fold and for $k_{r,ER}$, which decreased by half. No other variable changed by more than a factor of two (data not shown). These new parameter values did not improve the fit to the complete time-course. It is possible that Mg^{2+} concentrations less than 5 mM may be overestimated due to chelation of Mg^{2+} by ATP in the spectrophotometric assay solution (Ward and Keys, 1989) which may be the cause of model deviation from data in this range.

Given the fitted equilibrium constants, derived from fitted rate constants, we are now in a position to predict conditions under which full activation of RuBisCO is attained.

In the absence of RuBP and XuBP, and assuming that the concentration of enzyme is very small compared with C and M, the activation ratio at steady-state is given by:

$$\frac{[\mathrm{ECM}]_{eq}}{[\mathrm{E}]_{eq}+[\mathrm{EC}]_{eq}+[\mathrm{ECM}]_{eq}}=\frac{\frac{[\mathrm{E}]_{eq}[\mathrm{C}]_{eq}[\mathrm{M}]_{eq}}{K_{EC}K_{ECM}}}{[\mathrm{E}]_{eq}+\frac{[\mathrm{E}]_{eq}[\mathrm{C}]_{eq}}{K_{EC}}+\frac{[\mathrm{E}]_{eq}[\mathrm{C}]_{eq}[\mathrm{M}]_{eq}}{K_{EC}K_{ECM}}}=\frac{\frac{[\mathrm{C}]_{eq}[\mathrm{M}]_{eq}}{K_{EC}K_{ECM}}}{1+\frac{[\mathrm{C}]_{eq}}{K_{EC}}+\frac{[\mathrm{C}]_{eq}[\mathrm{M}]_{eq}}{K_{EC}K_{ECM}}}$$

The activation ratio expressed as a function of $[C]_{eq}$ and $[M]_{eq}$ is displayed in Fig. 5 (top left: [RuBP]=0 μM). It is seen here that beyond a given arc of moderate values for $[C]_{eq}$ and $[M]_{eq}$, close to 100% carbamylation can be expected, in line with experimental evidence.

Activation in the presence of RuBP may also be predicted. Again, if the concentration of enzyme is small in comparison with C, M and R, then, after Mate *et al.* (1996) (see Appendix):

$$\frac{[\mathrm{E}]_{active}}{[\mathrm{E}]_{total}}=\frac{1+\frac{[\mathrm{R}]_{eq}}{K_{ECMR}}\left(1+\frac{[\mathrm{C}]_{eq}}{K_{ECMRC}}\right)}{1+\frac{[\mathrm{R}]_{eq}}{K_{ECMR}}\left(1+\frac{[\mathrm{C}]_{eq}}{K_{ECMRC}}\right)+\frac{K_{ECM}}{[\mathrm{M}]_{eq}}\left(1+\frac{[\mathrm{R}]_{eq}}{K_{ECR}}+\frac{K_{EC}}{[\mathrm{C}]_{eq}}\left(1+\frac{[\mathrm{R}]_{eq}}{K_{ER}}\right)\right)}$$

Here, $[E]_{active}$ refers to all enzyme species with bound Mg^{2+}, i.e. [ECM]+[ECMR]+[ECMRC]. The concentration of RuBP free to participate in carboxylation is limited to that which is not bound to Mg^{2+} and is given by:

$$[\mathrm{R}]_{eq}=\frac{[\mathrm{R}]_{total}}{1+\frac{[\mathrm{M}]_{eq}}{K_{RM}}}$$

Figure 5 shows how RuBP behaves as both a positive and negative effector. At high [HCO_3^-], increasing [RuBP] increases the activation ratio of RuBisCO towards 100% while at low [HCO_3^-], increasing [RuBP] decreases the activation state of RuBisCO. The opposite is true of Mg^{2+}: at high [Mg^{2+}], increasing RuBP decreases the activation ratio.

Discussion

Model derived values for k_{cat}, $K_{M,C}$, $K_{M,RuBP}$ and activation constants reflect experimentally determined values

The model-derived values for k_{cat} ($3.3\pm0.5\ s^{-1}$) and $K_{M,C}$ (10 ± 4 μM) compare favourably with experimentally determined values for spinach RuBisCO (for a review see von Caemmerer, 2000). It should be noted that K_{ECMRC} ($=k_{r,ECMRC}/k_{f,ECMRC}=2.8\pm2.7$ μM) $<K_{M,C}$ which suggests that the binding of substrate CO_2 to the activated enzyme-RuBP complex should be tighter than predicted by the half-saturation constant, $K_{M,C}$, as would be expected if the turnover number (k_{cat}) is greater than the decarboxylation rate ($k_{r,ECMRC}$). This is contrary to typical Michaelis–Menten kinetics for other enzymes where the turnover number is

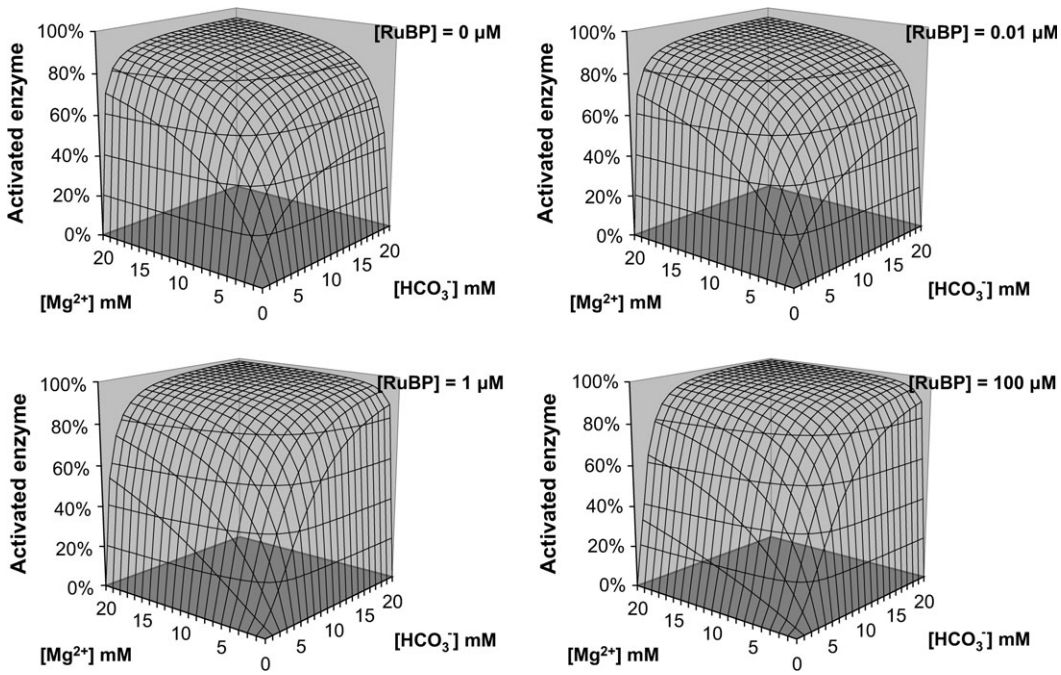

Fig. 5. Activated RuBisCO ([ECM]+[ECMR]+[ECMRC]) as a percentage of total enzyme and as a function of [HCO_3^-], [Mg^{2+}], and [RuBP], as predicted by the model of RuBisCO mechanism fitted at pH 8.0 and 25 °C. RuBP concentrations are 0 μM (top left), 0.01 μM (top right), 1 μM (bottom left), and 100 μM (bottom right).

much smaller than the back reaction rate from the Michaelis complex and where then the Michaelis–Menten half-saturation constant is equivalent to the binding affinity for the substrate.

The range of values for the apparent binding affinity constant for RuBP, $K_{M,RuBP}$ (1.5 ± 0.5 μM as $[CO_2] \rightarrow 0$ and 0.8 ± 0.2 μM as $[CO_2] \rightarrow \infty$) is close to experimentally determined values for spinach RuBisCO (2 μM) where chelation of RuBP with Mg^{2+} has been taken into account (Portis *et al*., 1995; von Caemmerer and Edmondson, 1986), as it has in this model. Note that the actual binding affinity constant for RuBP, K_{ECMR} (1.5 ± 0.5 μM) represents the upper limit for $K_{M,RuBP}$ as the concentration of CO_2 approaches its lower limit of zero. Both the binding affinity constant for binding of non-substrate CO_2 (K_{EC}: 200 ± 80 μM) and Mg^{2+} (K_{ECM}: 710 ± 210 μM), sometimes referred to as K_e and K_d elsewhere, are also close to the experimentally measured values for soybean (91 μM and 1130 μM, respectively) by Laing and Christeller (1976) and for spinach (309 μM and 529 μM, respectively) by Lorimer *et al*. (1976). The product $K_{EC}\times K_{ECM}\approx1.4\times10^5$ μM^2 is within the range of 1×10^5 μM^2–2×10^5 μM^2 calculated by Laing and Christeller (1976) and Lorimer *et al*. (1976) by different methods. This is the first time the kinetic constants for RuBisCO activation have been determined at 25 °C in the presence of RuBP.

Binding of RuBP to activated RuBisCO is fast and loose while binding to uncarbamylated enzyme is slow and tight

The RuBisCO active site lies at the interface of the N-terminal domain of one subunit and the loops connecting the strands of the C-terminal α/β-barrel of a neighbouring subunit (Spreitzer, 1993; Andersson and Taylor, 2003). Whereas carbamylation and chelation with Mg^{2+} induces minimal conformational change, binding of RuBP and other phosphorylated ligands induces a 12 Å shift in loop 6 of the α/β barrel from a retracted (open) position to an extended (closed) position and subsequent interaction with a short loop at the end of helix B of the N-terminal domain (Taylor and Andersson, 1996; Gutteridge and Gatenby, 1995). Loop 6 closes over the active site and reaction intermediate, shielding it from solvent so that only small molecules such as CO_2 and O_2 can gain access to the enediolate (Andrews, 1996). The (reverse) rate constant for decomposition of enzyme-bound RuBP (ECMR) to activated enzyme (ECM) and ligand (R), $k_{r,ECMR}$ (6.0 ± 1.5 s^{-1}) is of the same order as k_{cat} which is not surprising if it is considered that they may both be dictated by the same rate-limiting step: opening of loop 6 to release bound ligand from the activated enzyme.

The rate constant for decomposition of enzyme-bound XuBP (ECMX) to ECM and XuBP (X), $k_{r,ECMX}$ (0.075 ± 0.034 s^{-1}) is an order of magnitude smaller indicating that the inhibitor XuBP is released more slowly from activated enzyme than the substrate RuBP. The three rates for dissociation of sugar-bisphosphates from activated enzyme are all greater than those for dissociation of sugar bisphosphates from unactivated enzyme. These are the (reverse) rate constants for decomposition of free and carbamylated enzyme bound sugar bisphosphates (ER, EX, ECR, ECX) to enzymes (E, EC) and ligands (R, X). They include $k_{r,ER}$ (0.0018 ± 0.0012 s^{-1}), $k_{r,EX}$ (0.0007 ± 0.0003 s^{-1}), $k_{r,ECR}$ (0.028 ± 0.020 s^{-1}), and $k_{r,ECX}$ (0.0036 ± 0.0018 s^{-1}). This is consistent with a mechanism where binding of RuBP and XuBP to activated enzyme induces a faster opening of loop 6 than the binding of these ligands to unactivated enzyme where the resulting complex becomes somewhat 'locked'. This may well be one of the functions of the carbamate and/or the Mg^{2+} cofactor in the activated enzyme. It should be remembered that, if this binding process is biphasic as discussed in the Appendix, then the model-derived reverse rates are equivalent to the reverse rates for the slow-tight binding steps ($k_{r,EI*}$) (see Appendix) which may in turn represent the rate of opening of loop 6 (Pearce and Andrews, 2003).

The (forward) rate constants for association of enzymes and ligands to form enzyme–ligand complexes may also shed light on RuBisCO reaction mechanism. The rate-constants for binding of RuBP (R) and XuBP (X) to activated enzyme (ECM) to form bound sugar bisphosphate complexes (ECMR and ECMX, respectively) are $k_{f,ECMR}=(4300\pm900)$ mM^{-1} s^{-1} and $k_{f,ECMX}=(2800\pm1100)$ mM^{-1} s^{-1}, respectively. These are similar and much greater than the constants for binding of RuBP and XuBP to uncarbamylated enzyme (E) to form ER and EX given by $k_{f,ER}=(41\pm21$ mM^{-1} s^{-1} and $k_{f,EX}=22\pm8$ mM^{-1} s^{-1}, respectively. This is consistent with activated RuBisCO being more specific than uncarbamylated RuBisCO for the substrate, RuBP, and, incidentally, for its epimer, XuBP. For carbamylated (but not activated) RuBisCO, the situation is more ambiguous. The rate-constant for binding of XuBP to carbamylated enzyme (EC) ($k_{f,ECX}=2900\pm1100$ mM^{-1} s^{-1}) is fast while the rate constant for binding of RuBP to EC ($k_{f,ECR}=44\pm15$ mM^{-1} s^{-1}) is slow. The tight binding of XuBP to carbamylated enzyme may be an undesirable but unavoidable consequence of the functionality of the carbamate as the general base for enolization of substrate RuBP, as described by Cleland *et al*. (1998). It is, however, the addition of Mg^{2+} to the carbamate which seems to make RuBisCO highly specific for the substrate RuBP. Again, if the binding of sugar bisphosphates to RuBisCO is biphasic, then it is difficult to make any more than relative comparisons between individual forward rate constants (see Appendix).

The model-predicted forward and reverse rates for binding of sugar bisphosphates reveal a trend. While these ligands bind faster to activated enzyme, they are also

released faster. Conversely, while they bind more slowly to uncarbamylated enzyme, they are released more slowly. Intuitively, it would seem sensible for nature to select for an activated enzyme that binds substrate RuBP quickly and releases it slowly. It can be speculated that the reason this is not the case is as follows. As well as facilitating enolization, the formation at the active site of a carbamate with non-substrate CO_2 may have the undesirable but unavoidable consequence of increasing the rate of binding of the epimer, XuBP. In order to prevent choking of the active site with this inhibitor as a result of the misprotonation side reaction of enolized RuBP, it may be the role of Mg^{2+} not only to stabilize the carbamate but to facilitate the faster opening of loop 6 to release XuBP. This, of course, will have the disadvantage of releasing RuBP as well. This limitation may be an example of the competing demands placed on the RuBisCO enzyme as a result of its evolutionary history, similar to the inherent inefficiencies that are a result of the oxygenase reaction competing with the carboxylase reaction.

The equilibrium constants for binding of sugar bisphosphates to free, carbamylated, and activated RuBisCO reflect the individual forward and reverse rates for these processes. The model-predicted constants indicate that RuBP binds more tightly (but also more slowly) to uncarbamylated enzyme (K_{ER}=0.039±0.026 μM) than to activated enzyme (K_{ECMR}=1.5±0.5 μM) which corresponds with experimental data (Vater and Salnikow, 1979; Jordan and Chollet, 1983; Frank *et al*., 1998). However, XuBP binds equally tightly to the activated enzyme (K_{ECMX}=0.033±0.023 μM) and the uncarbamylated enzyme (K_{EX}=0.031±0.007 μM). Of these constants, it is only K_{ER} and K_{EX} that have been previously measured. The model-predicted range for K_{ER} encompasses the value measured by Jordan and Chollet (1983) (20 nM) even though this value is probably underestimated at 25 °C as it was measured at 2 °C. The binding constant for XuBP binding to free enzyme, K_{EX} (29 nM), is, however, less than that measured by Zhu and Jensen (1991) at pH 8.0 (350 nM).

Decarbamylation of RuBisCO occurs at low concentrations of CO_2 and Mg^{2+}

Under any given conditions, this model also provides predictions of the concentrations of individual enzyme species which would be difficult, if not impossible, to measure experimentally. While the total enzyme concentration can be measured *in vivo* and dictated *in vitro*, its constituents, with associated ligands, are more elusive. Consider, for example, the experimental transients for RuBisCO (activated and unactivated) in 2.5 mM HCO_3^- and 2 mM Mg^{2+} (Fig. 2, top) where incomplete initial activation might be expected because of these low concentrations, according to Fig. 5. The under-activated enzyme has 'fallen over' dramatically 10 min after the initiation of carboxylation while the initially unactivated enzyme maintains a constant rate. Figure 6 shows the model-predicted concentrations of sugar phosphates (in addition to PGA), uninhibited enzyme species, and inhibited enzyme species over the 60 min period of reaction. In accordance with Fig. 5, initial activation (to ECM) for the activated enzyme is less than 50% of the total enzyme active site concentration (~ 30 nM). Upon initiation of carboxylation by addition of RuBP at 30 min, about 50% of the RuBP is chelated with Mg^{2+} for both the activated and unactivated enzymes. It is only for the activated enzyme that a small amount of activated RuBisCO complexed with carboxylated RuBP (ECMRC) persists after 30 min. However, this is quickly replaced by unactivated RuBisCO complexed with RuBP (ER) as the enzyme decarbamylates and this leads to the observed fallover. For the unactivated enzyme, fallover occurs immediately and the rate of PGA formation is constant as a result. While the sum of all activated enzyme species ([ECM]+[ECMX]+[ECMR]+[ECMRC]) declines for the initially activated enzyme, it never rivals the uncarbamylated enzyme species ([E]+[EX]+[ER]) for the initially unactivated enzyme.

Compare this with the experimental transients for RuBisCO in 10 mM HCO_3^- and 25 mM Mg^{2+} (Fig. 2, bottom) where close to complete activation might be expected, according to Fig. 5. Here there is very little difference in the rate of PGA formation between the initially activated and unactivated enzymes (Fig. 7). As expected, initial activation (to ECM) for the activated enzyme is close to 100%. Because of the higher [Mg^{2+}], nearly all of the RuBP is chelated with Mg^{2+} after addition of RuBP. For both the activated and unactivated enzymes, about 50% of activated RuBisCO is initially complexed with carboxylated RuBP (ECMRC), but this is replaced by activated enzyme without RuBP ligands (ECM). This time, fallover of the activated enzyme is increasingly due to accumulation of XuBP at the active site (ECMX and ECX) as a result of misprotonation of the enediol intermediate. The unactivated enzyme, although initially inhibited by RuBP, is also subject to build-up of ECMX and ECX. Hence decarbamylation of RuBisCO, while pronounced at low [HCO_3^-] and [Mg^{2+}], is largely insignificant at higher concentrations.

It is speculated that fallover may be caused by different mechanisms under different circumstances. When concentrations of CO_2 and Mg^{2+} are low and initial activation is significantly less than 100%, as predicted by Fig. 5, then equilibrium favours the uncarbamylated enzyme and the onset of dead end inhibition (accumulation of ER), in accordance with the observations of Laing and Christeller (1976) and Jordan and Chollet (1983). When concentrations of CO_2 and Mg^{2+} are high and activation is closer to 100%, then equilibrium favours the fully activated enzyme and the accumulation of a catalytic side product (probably XuBP) at the active site. This supports the observations of Edmondson *et al*. (1990*b*, *c*, *d*) and Pearce and Andrews (2003). Very recently, Kim and Portis (2006) have

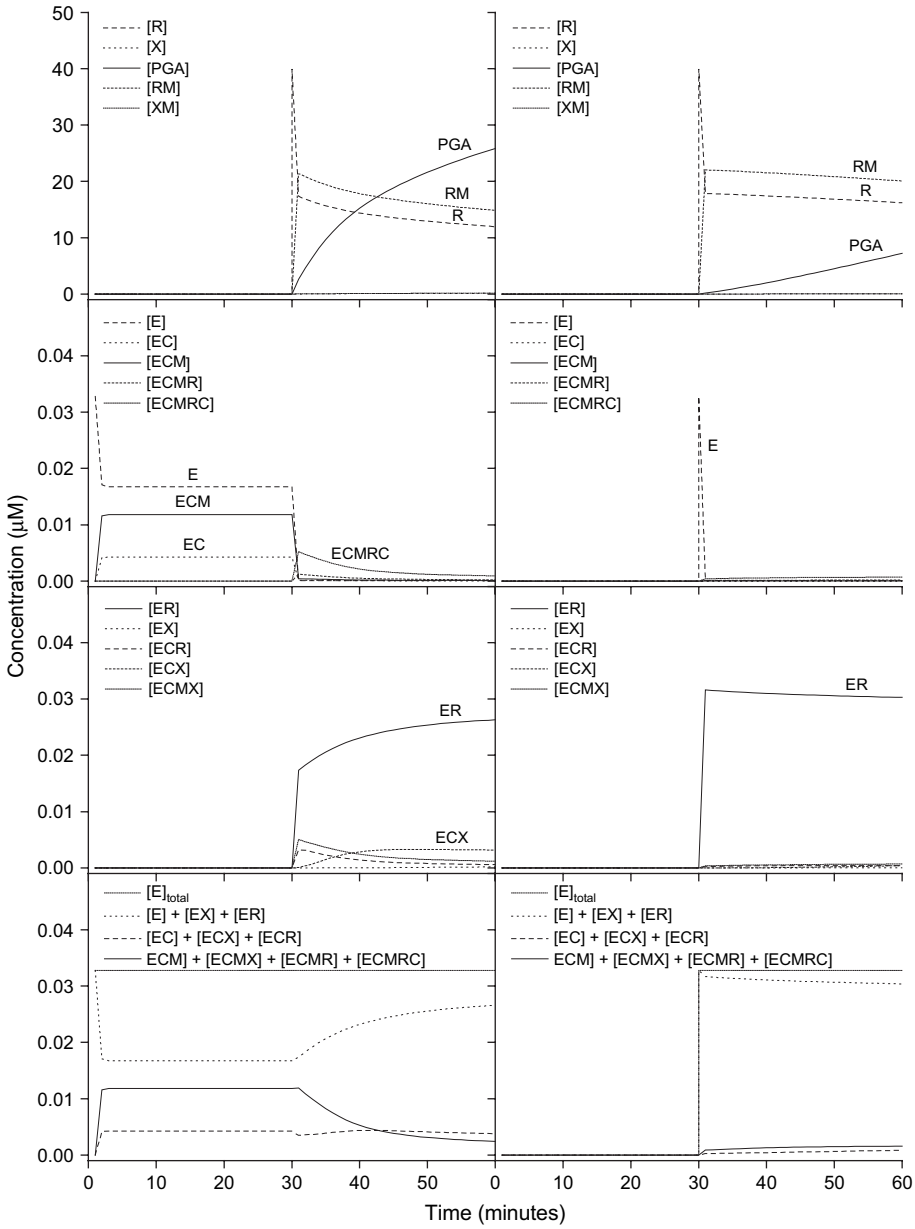

Fig. 6. Model-predicted outputs over the course of the 60 min reaction where carboxylation was initiated at 30 min. Initial conditions correspond to the data in Fig. 2 where the concentration of HCO_3^- was 2.5 mM and the concentration of Mg^{2+} was 2 mM. Prior to initiation of carboxylation by addition of RuBP, RuBisCO was either activated (left) or unactivated (right). Outputs include those for sugar phosphates (top row), uninhibited enzyme species (second row), inhibited enzyme species (third row), and enzyme carbamylation/activation status (bottom row).

validated these findings. They showed that slow inactivation of RuBisCO (fallover) was facilitated by low concentrations of both CO_2 and Mg^{2+} and that this was associated with a loss of carbamylation.

Activation of RuBisCO occurs in the presence of RuBP even though RuBP binds more tightly to uncarbamylated enzyme

Edmondson *et al*. (1990*b*) point to the apparent paradox that RuBisCO undergoes carbamylation at all when RuBP binds over 100-fold more tightly to the uncarbamylated enzyme than to the carbamylated form. It has been shown that this conflict may be resolved by considering the effects of non-substrate CO_2 and Mg^{2+} on activation. High concentrations of both of these 'push' RuBisCO towards the activated form. One cannot consider the relative binding affinities of RuBP alone in order to compare the energetically favoured enzyme state. The binding affinities of non-substrate CO_2 and Mg^{2+} must also be considered as well as the fact that, while RuBP binds more loosely to activated enzyme than to uncarbamylated enzyme, it binds more quickly.

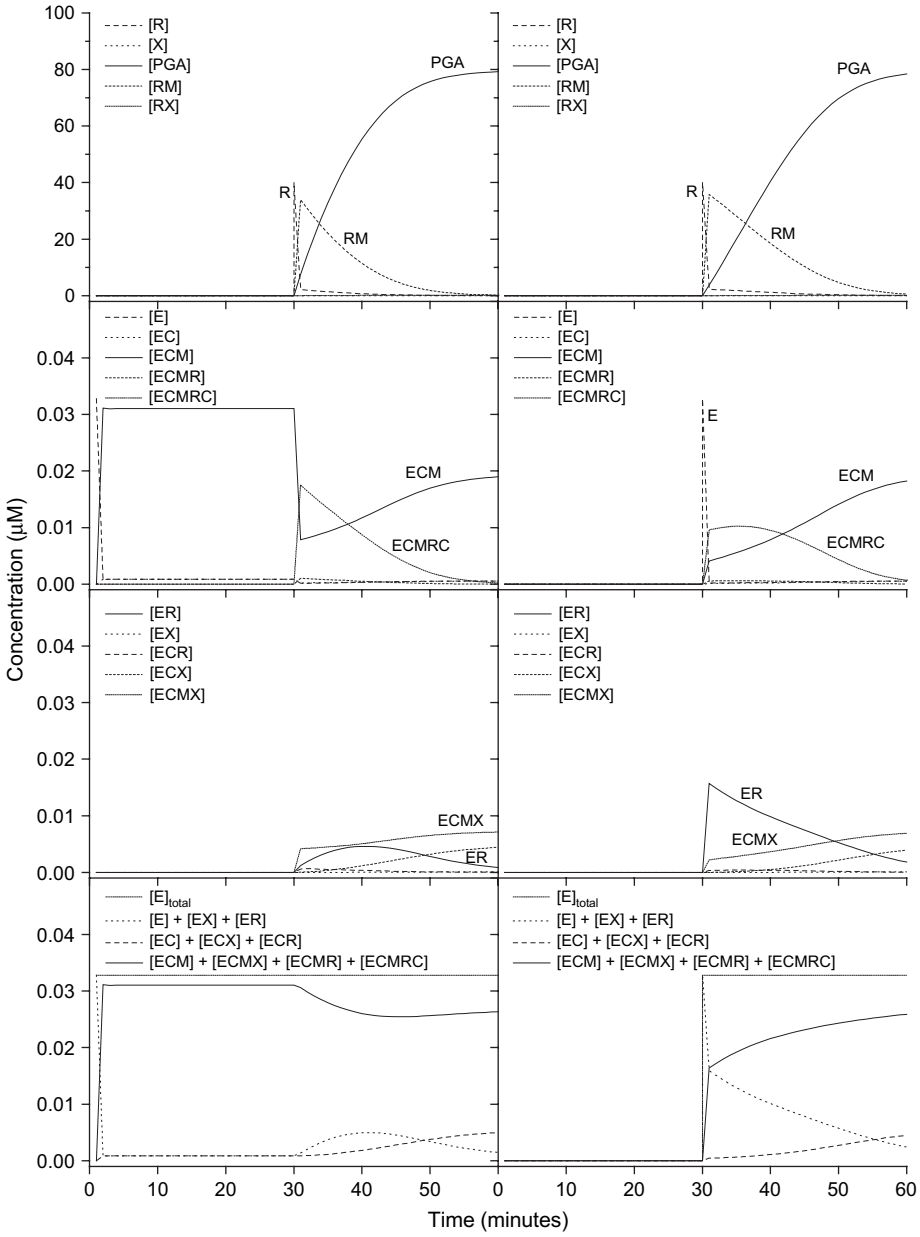

Fig. 7. Model-predicted outputs over the course of the 60 min reaction where carboxylation was initiated at 30 min. Initial conditions correspond to the data in Fig. 2 where the concentration of HCO_3^- was 10 mM and the concentration of Mg^{2+} was 25 mM. Prior to initiation of carboxylation by addition of RuBP, RuBisCO was either activated (left) or unactivated (right). Outputs include those for sugar phosphates (top row), uninhibited enzyme species (second row), inhibited enzyme species (third row), and enzyme carbamylation/activation status (bottom row).

Overall, the observations of Badger and Lorimer (1981) are pertinent here. They point out that the activity of RuBisCO will be governed by the relative ratios of the binding affinity constants of all the effectors in play. Jordan *et al*. (1983) point further to the complicating effects of concentration to explain why they found certain phosphates to be negative effectors when Badger and Lorimer found the same phosphates to be positive effectors. Indeed, it was found that at low CO_2 but high Mg^{2+} concentrations, RuBP is a negative effector while at high CO_2 and low Mg^{2+} concentrations it is a positive effector. When it is considered that this model and these experiments include the effectors RuBP and XuBP and their relative binding affinities to free enzyme, E, carbamylated enzyme, EC, and activated enzyme, ECM, the range of transient responses under a range of concentrations of these and other substrates is very wide indeed.

The decarboxylation rate

Pierce *et al*. (1986) provided evidence that the decarboxylation rate for RuBisCO was insignificant by showing that

partitioning of the 3-keto-CABP intermediate towards decarboxylation (as opposed to hydrolysis) by spinach RuBisCO was negligible. It should be noted, however, that Lorimer *et al.* (1986) showed that the enzyme-stabilized intermediate is the hydrated gem diol and not the 3-keto-CABP so the evidence is not conclusive. Although perhaps smaller than k_{cat}, the model-predicted rate constant for decarboxylation, $k_{r,ECMRC}$ (1.6 ± 1.1 s^{-1}), is non-zero which appears to be at odds with Pierce *et al.* (1986). However, given the uncertainties of the predicted rate constants, the commitment of the carboxylated intermediate towards decarboxylation could be as low as:

$$\frac{k_{r,ECMRC}}{k_{r,ECMRC}+k_{cat}}=\frac{(1.6-1.1)s^{-1}}{(1.6-1.1)s^{-1}+(3.3+0.5)s^{-1}}=0.12$$

The validity of our value for the decarboxylation rate was checked by reapplying our simultaneous multiple non-linear regression to the model using our model-predicted mean values for all rate-constants as a starting condition, except that $k_{r,ECMRC}$ was set to zero. This resulted in no improvement in the sum of residuals for any of the three sets of 18 experimental transients and yielded the new mean values for rate constants depicted in Fig. 8. These new values do not differ significantly from those in Fig. 3 (and remain within error bounds) which implies that the regression is not particularly sensitive to the rate of decarboxylation near zero. This model therefore does not necessarily support a significant decarboxylation rate, but it does suggest that this rate has a limited effect on the transient response of RuBisCO kinetics under the experimental conditions observed. The reason for this is that the concentrations of CO_2 employed experimentally were greater than the saturation concentration for binding of CO_2 to ECMR ($K_{ECMRC}=2.8\pm2.7$ μM). It is only at subsaturating concentrations of substrate CO_2 (<10 μM) that the kinetic response of RuBisCO is sensitive to the decarboxylation rate. Unfortunately, our experimental system is not sensitive enough to detect significant changes in PGA formation at subsaturating substrate CO_2 concentrations due to the virtually instant decarbamylation that occurs which in turn is a result of inadequate activation of RuBisCO.

Applicability of the modelling technique

It is recognized that this modelling technique provides better estimates of some constants than others. Because $[HCO_3^-]$ and $[Mg^{2+}]$ have been varied and a known concentration of RuBP has been introduced to a known concentration of activated and unactivated enzyme, it is expected that our estimates of equilibrium constants involving these species (e.g. K_{ER}, K_{EC}, K_{ECM}, K_{ECMR}, K_{ECMRC}) will be better than those which involve a species like XuBP which was not measured directly (e.g. K_{EX}, K_{ECX}, K_{ECMX}). Nevertheless, because 20 rate-constants have been fitted to 18 experimental transients, we are confident that most rate-constants are either accurate or have little effect on RuBisCO kinetics in the concentration ranges employed here. This is not to say that the values of some rate (and equilibrium) constants could not be refined under other experimental conditions where the concentration of XuBP, for example, is varied. Of course, the more data to which the model is fitted, the more confident we may be of these estimates.

Parameters associated with oxygenase activity have not been determined here, even though they will be significant under most physiological conditions. These will include a forward and reverse rate of oxygenation as well as a rate of formation of the potent inhibitor PDBP which, like XuBP, will bind to carbamylated and uncarbamylated active sites, resulting in fallover. To reduce the number of parameters to be fitted to experimental data they were excluded, but the

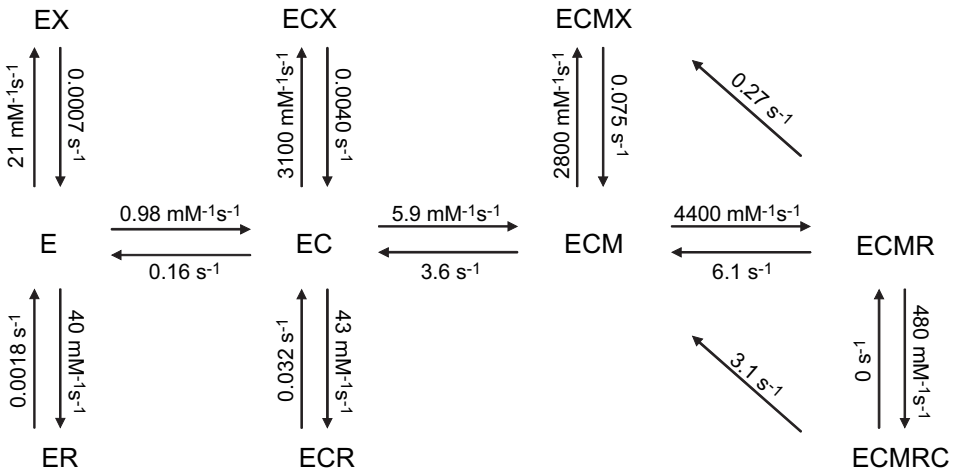

Fig. 8. Forward rates (mM^{-1} s^{-1}) and reverse rates (s^{-1}) that best fit the RuBisCO model to the 3×18 experimental transients at pH 8.0 and 25 °C when the rate of decarboxylation, $k_{r,ECMRC}$, is held at zero.

model is easily adjusted to account for them (see Appendix). Experimental data with at least two oxygen concentrations (e.g. zero and air-equilibrated) would need to be generated.

While multiple non-linear regression have been used to model the RuBisCO reaction mechanism, the technique could equally be applied to other enzyme kinetic models and, indeed, to any complex, non-linear metabolic pathway or process where limited data exist that do not directly measure a suite of hidden variables. The technique relies on the fact that complex, non-linear systems have multiple interdependencies embedded within them such that knowledge of the dynamics of a few of these variables constrains the dynamics of the remaining hidden variables within a model of the system to a finite set of possibilities. If enough variables are known or measured and enough data collected, the variables are limited to a unique solution. The more interconnected the system (and model), the fewer variables need to be directly measured and the fewer data need to be collected.

Conclusions

The 'fitted' model of RuBisCO reaction mechanism presented here provides dynamic rate constants and equilibrium binding affinity constants that agree with many previously measured values. In addition, these constants were obtained from an experimental method that is easily performed in one week. This method does not require the isolation of individual reaction steps that is needed for traditional methods. These data have then been used to shed light on aspects of RuBisCO kinetics. In particular, it is demonstrated that kinetic data are consistent with fast, loose binding of RuBP to activated RuBisCO while binding to uncarbamylated enzyme is slow and tight. This can explain why activation of RuBisCO occurs in the presence of RuBP even though RuBP binds more tightly to uncarbamylated enzyme. We contend that at low concentrations of CO_2 and Mg^{2+}, decarbamylation of RuBisCO is followed by dead end inhibition as RuBP binds to the uncarbamylated enzyme active sites.

Supplementary data

The MATLAB code for the three function files described in this paper are included at JXB online as supplementary material. These are: the function containing the differential mass balance equations which describe RuBisCO kinetics in the form $d\mathbf{y}/dt=f(\mathbf{y},\mathbf{k})$ (Rkinetics.m), the function that integrates the system of differential equations in the form $\mathbf{y}=f(t,\mathbf{k})$ (Rintegrate.m) and the supervising function that applies non-linear least squares curve fitting to the integrated model output (Rcurvefit.m). Curve-fitting is performed by running the supervising program which then calls the other functions as subroutines. The functions periodically update a spreadsheet (Rdata.xls) with the best fit of model-generated output as well as the values of fitted constants at each iteration. Two MATLAB-supplied functions are also used: an ordinary differential equation solver (ode15s.m) and a non-linear least-squares curve-fitting algorithm (lsqcurvefit.m), available in the MATLAB Optimization Toolbox. The regression generally requires more than 1 d to converge to a suitable solution on a desktop PC and is terminated by 'Ctrl-C'.

Acknowledgements

The multiple non-linear regression was performed using MATLAB software (MathWorks, 2002) on a 2.66 GHz Pentium 4 CPU as part of the Linux Cluster operated by the National Facility of the Australian Partnership for Advanced Computing (APAC) at the Australian National University (ANU). We also thank Professor T John Andrews for valuable advice on the catalytic mechanism of RuBisCO and Dr Heather Kane for valuable assistance in the laboratory. GDF thanks the Australian Research Council for funding support.

Appendix

The model is based on the assumption that the catalytic sites act independently of each other and that binding at one of the eight catalytic sites on the RuBisCO holoenzyme does not influence binding at another site (von Caemmerer, 2000). This may not be true for binding of sugar bisphosphates but it will be shown that biphasic binding can be condensed to a mathematically equivalent single step. With respect to carboxylation, bound RuBP is deprotonated (enolization) before carboxylation proceeds by way of a sequential reaction involving addition of CO_2 to form a ketone intermediate; hydration to form a gem diol and proton abstraction and cleavage of the intermediate to form two molecules of PGA (Pierce *et al*., 1980; Andrews and Lorimer, 1987; Cleland *et al*., 1998). While Lorimer *et al*. (1986) provide evidence that the intermediate is stabilized at the active site as the hydrated gem diol, the form of the carboxylation intermediate is not distinguished, whether it be the 3-keto-CABP form or the gem diol form. In the former case, hydration and cleavage are collapsed into a single step and in the latter case carboxylation and hydration are collapsed into a single step. No attempt has been made to disentangle these individual steps, but only to quantify the rate-limiting step in each case.

Mass balances

The mass balances for each of the enzyme species (Fig. 1) are as follows:

$$\frac{d[E]}{dt} = v_{r,EC} - v_{f,EC} + v_{r,ER} - v_{f,ER} + v_{r,EX} - v_{f,EX} \quad (1)$$

$$\frac{d[EX]}{dt} = v_{f,EX} - v_{r,EX} \quad (2)$$

$$\frac{d[ER]}{dt} = v_{f,ER} - v_{r,ER} \quad (3)$$

$$\frac{d[EC]}{dt} = v_{f,EC} - v_{r,EC} + v_{r,ECM} - v_{f,ECM} + v_{r,ECR} - v_{f,ECR} + v_{r,ECX} - v_{f,ECX} \quad (4)$$

$$\frac{d[ECX]}{dt} = \nu_{f,ECX} - \nu_{r,ECX} \quad (5)$$

$$\frac{d[ECR]}{dt} = \nu_{f,ECR} - \nu_{r,ECR} \quad (6)$$

$$\frac{d[ECM]}{dt} = \nu_{f,ECM} - \nu_{r,ECM} + \nu_{r,ECMR} - \nu_{f,ECMR} + \nu_{r,ECMX} - \nu_{f,ECMX} + \nu_{cat} \quad (7)$$

$$\frac{d[ECMX]}{dt} = \nu_{f,ECMX} - \nu_{r,ECMX} + \nu_{mis} \quad (8)$$

$$\frac{d[ECMR]}{dt} = \nu_{f,ECMR} - \nu_{r,ECMR} + \nu_{r,ECMRC} - \nu_{f,ECMRC} - \nu_{mis} \quad (9)$$

$$\frac{d[ECMRC]}{dt} = \nu_{f,ECMRC} - \nu_{r,ECMRC} - \nu_{cat} \quad (10)$$

The substrate for carboxylation, C (CO_2), is in equilibrium with HCO_3^- and CO_3^{2-}. Hence the mass balances for C and its derivatives are determined by acid base equilibria where:

$$\frac{[HCO_3^-][H^+]}{[CO_2]} = K_{CO2} = 10^{-6.25} = 5.62\times10^{-7}\,M$$

$$\frac{[CO_3^{2-}][H^+]}{[HCO_3^-]} = K_{HCO3} = 10^{-10.33} = 4.67\times10^{-11}\,M$$

Then:

$$\frac{d[C]}{dt} + \frac{d[HCO_3^-]}{dt} + \frac{d[CO_3^{2-}]}{dt} = \nu_{r,EC} - \nu_{f,EC} + \nu_{r,ECMRC} - \nu_{f,ECMRC}$$

Substituting equilibrium expressions:

$$\frac{d[C]}{dt} = \frac{\nu_{r,EC} - \nu_{f,EC} + \nu_{r,ECMRC} - \nu_{f,ECMRC}}{1 + \frac{K_{CO2}}{[H^+]} + \frac{K_{CO2}K_{HCO3}}{[H^+]^2}} \quad (11)$$

Sugar bisphosphates form a complex with magnesium in solution (Martell and Calvin, 1952). The complex formed between R and M is described by:

$$R + M \underset{k_{r,RM}}{\overset{k_{f,RM}}{\rightleftharpoons}} RM + M \underset{k_{r,RM_2}}{\overset{k_{f,RM_2}}{\rightleftharpoons}} RM_2 - M - M$$

The first equilibrium is defined by (von Caemmerer and Edmondson, 1986; von Caemmerer and Farquhar, 1985):

$$\frac{[R][M]}{[RM]} = K_{RM} = 0.0016\,M$$

The second equilibrium results in negligible RM_2 (i.e. $\upsilon_{f,RM2} \approx \upsilon_{r,RM2} \approx 0$). It is assumed that the binding of M to the other sugar bisphosphate, X, can be described by the same equilibrium constant (i.e. K_{XM}=0.0016 M). Hence the mass balances for R, X, M, RM and XM are given by:

$$\frac{d[R]}{dt} = \nu_{r,ER} - \nu_{f,ER} + \nu_{r,ECR} - \nu_{f,ECR} + \nu_{r,ECMR} - \nu_{f,ECMR} + \nu_{r,RM} - \nu_{f,RM} \quad (12)$$

$$\frac{d[X]}{dt} = \nu_{r,EX} - \nu_{f,EX} + \nu_{r,ECX} - \nu_{f,ECX} + \nu_{r,ECMX} - \nu_{f,ECMX} + \nu_{r,XM} - \nu_{f,XM} \quad (13)$$

$$\frac{d[M]}{dt} = \nu_{r,ECM} - \nu_{f,ECM} + \nu_{r,RM} - \nu_{f,RM} + \nu_{r,XM} - \nu_{f,XM} \quad (14)$$

$$\frac{d[RM]}{dt} = \nu_{f,RM} - \nu_{r,RM} \quad (15)$$

$$\frac{d[XM]}{dt} = \nu_{f,XM} - \nu_{r,XM} \quad (16)$$

The remaining mass balance describing formation of the reaction product is:

$$\frac{d[PGA]}{dt} = 2\nu_{cat} \quad (17)$$

Rate expressions

The molar reaction rates included in the mass balances may be defined as follows:

$$\nu_{cat} = k_{cat}[ECMRC]$$

$$\nu_{mis} = k_{mis}[ECMR]$$

$$\nu_{f,ECMRC} = k_{f,ECMRC}[ECMR][C]$$

$$\nu_{r,ECMRC} = k_{r,ECMRC}[ECMRC]$$

$$\nu_{f,ECMR} = k_{f,ECMR}[ECM][R]$$

$$\nu_{r,ECMR} = k_{r,ECMR}[ECMR]$$

$$\nu_{f,ECMX} = k_{f,ECMX}[ECM][X]$$

$$\nu_{r,ECMX} = k_{r,ECMX}[ECMX]$$

$$\nu_{f,ECM} = k_{f,ECM}[EC][M]$$

$$\nu_{r,ECM} = k_{r,ECM}[ECM]$$

$$\nu_{f,ECX} = k_{f,ECX}[EC][X]$$

$$\nu_{r,ECX} = k_{r,ECX}[ECX]$$

$$\nu_{f,ECR} = k_{f,ECR}[EC][R]$$

$$\nu_{r,ECR} = k_{r,ECR}[ECR]$$

$$v_{f,EC} = k_{f,EC}[E][C]$$

$$v_{r,EC} = k_{r,EC}[EC]$$

$$v_{f,EX} = k_{f,EX}[E][X]$$

$$v_{r,EX} = k_{r,EX}[EX]$$

$$v_{f,ER} = k_{f,ER}[E][R]$$

$$v_{r,ER} = k_{r,ER}[ER]$$

$$v_{f,RM} = k_{f,RM}[R][M]$$

$$v_{r,RM} = k_{r,RM}[RM]$$

$$v_{f,XM} = k_{f,XM}[X][M]$$

$$v_{r,XM} = k_{r,XM}[XM]$$

The rate constants $k_{f,RM}$, $k_{r,RM}$, $k_{f,XM}$, and $k_{r,XM}$ are related by the imposed constraints (von Caemmerer and Edmondson, 1986):

$$\frac{k_{r,RM}}{k_{f,RM}} = k_{RM} = 0.0016\,M$$

$$\frac{k_{r,XM}}{k_{f,XM}} = k_{XM} = 0.0016\,M$$

It is acknowledged that binding of RuBP and other sugar bisphosphates to RuBisCO appears to be biphasic, indicating either negative co-operativity (Frank *et al*., 1998) or two stage binding (fast-loose binding followed by slow-tight binding) (Pierce *et al*., 1980; Jordan and Chollet, 1983; Zhu and Jensen, 1991; Pearce and Andrews, 2003) according to:

$$E + I \underset{k_{r,EI}}{\overset{k_{f,EI}}{\rightleftharpoons}} EI \underset{k_{r,EI*}}{\overset{k_{f,EI*}}{\rightleftharpoons}} EI*$$

However, mass balances on the enzyme–inhibitor complexes can be shown to result in mathematically equivalent overall forward and reverse rates and an overall equilibrium constant as follows:

$$\frac{d[EI*]}{dt} = k_{f,EI*}[EI] - k_{r,EI*}[EI*]$$

At steady-state:

$$\frac{d[EI*]}{dt} = k_{f,EI*}[EI]_{eq} - k_{r,EI*}[EI*]_{eq} = 0$$

Therefore:

$$k_{f,EI*}[EI]_{eq} = k_{r,EI*}[EI*]_{eq}$$

$$\frac{k_{r,EI*}}{k_{f,EI*}} = \frac{[EI]_{eq}}{[EI*]_{eq}} = K_{EI*}$$

Now, also at steady-state:

$$\frac{d[EI]}{dt} = k_{f,EI}[E]_{eq}[I]_{eq} - k_{r,EI}[EI]_{eq} - k_{f,EI*}[EI]_{eq} + k_{r,EI*}[EI*]_{eq} = 0$$

Therefore:

$$k_{f,EI}[E]_{eq}[I]_{eq} = k_{r,EI}[EI]_{eq}$$

$$\frac{k_{r,EI}}{k_{f,EI}} = \frac{[E]_{eq}[I]_{eq}}{[EI]_{eq}} = K_{EI}$$

Now:

$$\frac{d[EI*]}{dt} = \frac{k_{f,EI*}}{K_{EI}}[E][I] - k_{r,EI*}[EI*]$$

At steady-state:

$$\frac{d[EI*]}{dt} = \frac{k_{f,EI*}}{K_{EI}}[E]_{eq}[I]_{eq} - k_{r,EI*}[EI*]_{eq} = 0$$

$$\frac{k_{f,EI*}}{K_{EI}}[E]_{eq}[I]_{eq} = k_{r,EI*}[EI*]_{eq}$$

$$\frac{[E]_{eq}[I]_{eq}}{[EI*]_{eq}} = \frac{k_{r,EI*}}{K_{f,EI*}/K_{EI}} = K_{EI}\frac{k_{r,EI*}}{K_{f,EI*}} = K_{EI}K_{EI*} = K_{overall}$$

where the overall reverse rate is equal to the reverse rate for the slow-tight binding ($k_{r,EI*}$) and the overall forward rate is given by $k_{f,EI*}/K_{EI}$.

Thus the complete mathematical model consists of 17 differential mass balances in 17 variables describing the fates of 17 species in solution: E, ER, EX, EC, ECR, ECX, ECM, ECMR, ECMX, ECMRC, C, R, X, M, RM, XM, PGA. The initial concentrations of each species must be specified in order to identify a numerical solution. There are 20 unknown rate constants to be 'fitted' to the experimental data: k_{cat}, k_{mis}, $k_{f,ECMRC}$, $k_{r,ECMRC}$, $k_{f,ECMR}$, $k_{r,ECMR}$, $k_{f,ECMX}$, $k_{r,ECMX}$, $k_{f,ECM}$, $k_{r,ECM}$, $k_{f,ECX}$, $k_{r,ECX}$, $k_{f,ECR}$, $k_{r,ECR}$, $k_{f,EC}$, $k_{r,EC}$, $k_{f,EX}$, $k_{r,EX}$, $k_{f,ER}$, $k_{r,ER}$. Either one of $k_{f,RM}$ or $k_{r,RM}$ and either one of $k_{f,XM}$ or $k_{r,XM}$ must also be fitted but, by setting these to very high values, they are fixed and a system is described where chelation of Mg^{2+} with RuBP and XuBP is instantaneous. Knowledge of the rate constants then enables calculation of the nine equilibrium (binding affinity) constants, K_{ECMRC}, K_{ECMR}, K_{ECMX}, K_{ECM}, K_{ECX}, K_{ECR}, K_{EC}, K_{EX}, K_{ER}, where the binding constant for each equilibrium step is the reverse rate constant for that step divided by the forward rate constant for the same step.

Oxygenase activity

The model presented thus far neglects oxygenase activity and assumes that experimental data are generated in oxygen-free conditions. The presence of oxygen requires that the model be augmented with mass balances for oxygen; the peroxyketone reaction intermediate; the oxygenation product 2PG; the oxygenase-related inhibitor PDBP; PDBP bound to uncarbamylated, carbamylated, and fully activated enzyme; and PDBP bound to Mg^{2+}. These and other mass balances will then need to incorporate rate expressions for hydration/cleavage of the peroxyketone intermediate; the H_2O_2 elimination reaction forming PDBP; binding and dissociation of oxygen to and from enzyme-bound RuBP; binding and dissociation of PDBP to and from uncarbamylated, carbamylated, and fully activated enzyme; and binding and dissociation of Mg^{2+} to PDBP.

Activation ratio

After Mate *et al*. (1996), the total enzyme site concentration in the absence of XuBP is given by:

$$[E]_{total} = [E] + [ER] + [EC] + [ECR] + [ECM] + [ECMR] + [ECMRC]$$

If the concentration of enzyme is small in comparison with [C], [M] and [R], then at equilibrium:

$$[E]_{total,eq} = [E]_{eq}\left(1 + \frac{[R]_{eq}}{K_{ER}} + \frac{[C]_{eq}}{K_{EC}} + \frac{[C]_{eq}[R]_{eq}}{K_{EC}K_{ECR}} + \frac{[C]_{eq}[M]_{eq}}{K_{EC}K_{ECM}} + \frac{[C]_{eq}[M]_{eq}[R]_{eq}}{K_{EC}K_{ECM}K_{ECMR}} + \frac{[C]_{eq}^2[M]_{eq}[R]_{eq}}{K_{EC}K_{ECM}K_{ECMR}K_{ECMRC}}\right)$$

The sum of the concentrations of activated enzyme species is:

$$[E]_{active} = [ECM] + [ECMR] + [ECMRC] = [E]_{eq}\left(\frac{[C]_{eq}[M]_{eq}}{K_{EC}K_{ECM}} + \frac{[C]_{eq}[M]_{eq}[R]_{eq}}{K_{EC}K_{ECM}K_{ECMR}} + \frac{[C]_{eq}^2[M]_{eq}[R]_{eq}}{K_{EC}K_{ECM}K_{ECMR}K_{ECMRC}}\right)$$

The activation ratio is then given by:

$$\frac{[E]_{active}}{[E]_{total}} = \frac{1 + \frac{[R]_{eq}}{K_{ECMR}}\left(1 + \frac{[C]_{eq}}{K_{ECMRC}}\right)}{1 + \frac{[R]_{eq}}{K_{ECMR}}\left(1 + \frac{[C]_{eq}}{K_{ECMRC}}\right) + \frac{K_{ECM}}{[M]_{eq}}\left(1 + \frac{[R]_{eq}}{K_{ECR}} + \frac{K_{EC}}{[C]_{eq}}\left(1 + \frac{[R]_{eq}}{K_{ER}}\right)\right)}$$

Now, assuming that the fraction of R bound to enzyme is small, account must only be taken of the binding of R to M such that, if [M] is much greater than [R]:

$$K_{RM} = \frac{[R]_{eq}[M]_{eq}}{[RM]_{eq}}$$

The total amount of RuBP is then:

$$[R]_{total} = [R]_{eq} + [RM]_{eq} = [R]_{eq} + \frac{[R]_{eq}[M]_{eq}}{K_{RM}} = [R]_{eq}\left(1 + \frac{[M]_{eq}}{K_{RM}}\right)$$

The concentration of RuBP free to participate in carboxylation is given by:

$$[R]_{eq} = \frac{[R]_{total}}{1 + \frac{[M]_{eq}}{K_{RM}}}$$

References

Andersson I, Taylor TC. 2003. Structural framework for catalysis and regulation in ribulose-1, 5-*bis*phosphate carboxylase/oxygenase. *Archives of Biochemistry and Biophysics* **414,** 130–140.

Andrews TJ. 1996. The bait in the rubisco mousetrap. *Nature Structural Biology* **3,** 3–7.

Andrews TJ, Lorimer GH. 1987. Rubisco: structure, mechanisms, and prospects for improvement. In: Hatch MD, Boardman NK, eds. *The biochemistry of plants: a comprehensive treatise,* Vol. 10 *Photosynthesis*. New York: Academic Press, 131–218.

Andrews TJ, Whitney SM. 2003. Manipulating ribulose bisphosphate carboxylase/oxygenase in the chloroplasts of higher plants. *Archives of Biochemistry and Biophysics* **414,** 159–169.

Badger MR, Collatz GJ. 1977. Studies on the kinetic mechanism of RuBP carboxylase and oxygenase reactions, with particular reference to the effect of temperature on kinetic parameters. *Carnegie Institute Year Book* **76,** 355–361.

Badger MR, Lorimer GH. 1981. Interaction of sugar phosphates with the catalytic site of ribulose-1,5-*bis*phosphate carboxylase. *Biochemistry* **20,** 2219–2225.

Chen Y-R, Hartman FC. 1995. A signature of the oxygenase intermediate in catalysis by ribulose-*bis*phosphate carboxylase/oxygenase as provided by a site-directed mutant. *Journal of Biological Chemistry* **270,** 11741–11744.

Cleland WW, Andrews TJ, Gutteridge S, Hartman FC, Lorimer GH. 1998. Mechanism of rubisco: the carbamate as general base [review]. *Chemical Reviews* **98,** 549–561.

Coleman TF, Li YY. 1996. An interior trust region approach for nonlinear minimization subject to bounds. *Siam Journal on Optimization* **6,** 418–445.

Edmondson DL, Badger MR, Andrews TJ. 1990*a*. A kinetic characterization of slow inactivation of ribulose *bis*phosphate carboxylase during catalysis. *Plant Physiology* **93,** 1376–1382.

Edmondson DL, Badger MR, Andrews TJ. 1990*b*. Slow inactivation of ribulose *bis*phosphate carboxylase during catalysis is not due to decarbamylation of the catalytic site. *Plant Physiology* **93,** 1383–1389.

Edmondson DL, Badger MR, Andrews TJ. 1990*c*. Slow inactivation of ribulose *bis*phosphate carboxylase during catalysis is caused by accumulation of a slow, tight-binding inhibitor at the catalytic site. *Plant Physiology* **93,** 1390–1397.

Edmondson DL, Kane HJ, Andrews TJ. 1990*d*. Substrate isomerization inhibits ribulose *bis*phosphate carboxylase-oxygenase during catalysis. *FEBS Letters* **260,** 62–66.

Farquhar GD. 1979. Models describing the kinetics of ribulose biphosphate carboxylase-oxygenase. *Archives of Biochemistry and Biophysics* **193,** 456–468.

Frank J, Vater J, Holzwarth JF. 1998. Thermodynamics and kinetics of sugar phosphate binding to D-ribulose-1,5-*bis*phosphate carboxylase/oxygenase (RUBISCO). *Journal of the Chemical Society-Faraday Transactions* **94,** 2127–2133.

Gutteridge S, Gatenby AA. 1995. Rubisco synthesis, assembly, mechanism, and regulation. *The Plant Cell* **7,** 809–819.

Hall NP, Tolbert NE. 1978. Rapid procedure for isolation of ribulose bisphosphate carboxylase-oxygenase from spinach leaves. *FEBS Letters* **96,** 167–169.

Hatch AL, Jensen RG. 1980. Regulation of ribulose-1,5-*bis*phosphate carboxylase from tobacco: changes in pH response and affinity for CO_2 and Mg^{2+} induced by chloroplast intermediates. *Archives of Biochemistry and Biophysics* **205,** 587–594.

Horecker BL, Hurwitz J, Weissbach A. 1958. Ribulose diphosphate. In: Vestling CS, ed. *Biochemical preparations*, Vol. 6. New York: J Wiley & Sons, 83–90.

Jordan DB, Chollet R. 1983. Inhibition of ribulose *bis*phosphate carboxylase by substrate ribulose-1,5-*bis*phosphate. *Journal of Biological Chemistry* **258,** 13752–13758.

Jordan DB, Chollet R, Ogren WL. 1983. Binding of phosphorylated effectors by active and inactive forms of ribulose-1,5-*bis*phosphate carboxylase. *Biochemistry* **22,** 3410–3418.

Kim K, Portis AR. 2004. Oxygen-dependent H_2O_2 production by rubisco. *FEBS Letters* **571,** 124–128.

Kim K, Portis AR. 2006. Kinetic analysis of the slow inactivation of Rubisco during catalysis: effects of temperature, O_2 and Mg^{2+}. *Photosynthesis Research* **87,** 195–204.

Laing WA, Christeller JT. 1976. Model for kinetics of activation and catalysis of ribulose 1,5-*bis*phosphate carboxylase. *Biochemical Journal* **159,** 563–570.

Leatherbarrow RJ. 1990. Using linear and non-linear regression to fit biochemical data. *Trends in Biochemical Sciences* **15,** 455–458.

Lilley RM, Walker DA. 1974. Improved spectrophotometric assay for ribulose-*bis*phosphate carboxylase. *Biochimica et Biophysica Acta* **358,** 226–229.

Lorimer GH, Andrews TJ, Pierce J, Schloss JV. 1986. 2′-carboxy-3-keto-D-arabinitol 1,5-*bis*phosphate, the six-carbon intermediate of the ribulose *bis*phosphate carboxylase reaction. *Philosophical Transactions of the Royal Society of London Series B-Biological Sciences* **313,** 397–407.

Lorimer GH, Badger MR, Andrews TJ. 1976. The activation of ribulose-1,5-*bis*phosphate carboxylase by carbon dioxide and magnesium ions. Equilibria, kinetics, a suggested mechanism and physiological implications. *Biochemistry* **15,** 529–536.

Martell AE, Calvin M. 1952. *Chemistry of the metal chelate compounds*. New York: Prentice-Hall.

Mate CJ, von Caemmerer S, Evans JR, Hudson GS, Andrews TJ. 1996. The relationship between CO_2-assimilation rate, rubisco carbamylation and rubisco activase content in activase-deficient transgenic tobacco suggests a simple model of activase action. *Planta* **198,** 604–613.

MathWorks. 2002. *MATLAB*. Natick, MA: The MathWorks, Inc.

McCulloch AD, Huber G. 2002. Integrative biological modelling *in silico*. In: Bock G, Goode JA, eds. 'In silico' *simulation of biological processes*, Vol. 6. John Wiley & Sons Ltd, 4–25.

Morell MK, Wilkin JM, Kane HJ, Andrews TJ. 1997. Side reactions catalyzed by ribulose-*bis*phosphate carboxylase in the presence and absence of small subunits. *Journal of Biological Chemistry* **272,** 5445–5451.

Parry MAJ, Andralojc PJ, Mitchell RAC, Madgwick PJ, Keys AJ. 2003. Manipulation of rubisco: the amount, activity, function and regulation. *Journal of Experimental Botany* **54,** 1321–1333.

Pearce FG, Andrews TJ. 2003. The relationship between side reactions and slow inhibition of ribulose-biphosphate carboxylase revealed by a loop 6 mutant of the tobacco enzyme. *Journal of Biological Chemistry* **278,** 32526–32536.

Peck SL. 2004. Simulation as experiment: a philosophical reassessment for biological modeling. *Trends in Ecology and Evolution* **19,** 530–534.

Pierce J, Andrews TJ, Lorimer GH. 1986. Reaction intermediate partitioning by ribulose-*bis*phosphate carboxylases with differing substrate specificities. *Journal of Biological Chemistry* **261,** 248–256.

Pierce J, Tolbert NE, Barker R. 1980. Interaction of ribulose *bis*phosphate carboxylase-oxygenase with transition-state analogs. *Biochemistry* **19,** 934–942.

Portis AR. 2003. Rubisco activase: Rubisco's catalytic chaperone. *Photosynthesis Research* **75,** 11–27.

Portis AR, Lilley RM, Andrews TJ. 1995. Subsaturating ribulose-1,5-*bis*phosphate concentration promotes inactivation of ribulose-1,5-*bis*phosphate carboxylase/oxygenase (rubisco): studies using continuous substrate addition in the presence and absence of rubisco activase. *Plant Physiology* **109,** 1441–1451.

Shampine LF, Reichelt MW. 1997. The MATLAB ODE suite. *Siam Journal on Scientific Computing* **18,** 1–22.

Spreitzer RJ. 1993. Genetic dissection of rubisco structure and function. *Annual Review of Plant Physiology and Plant Molecular Biology* **44,** 411–434.

Spreitzer RJ, Salvucci ME. 2002. Rubisco: structure, regulatory interactions, and possibilities for a better enzyme. *Annual Review of Plant Biology* **53,** 449–475.

Taylor TC, Andersson I. 1996. Structural transitions during activation and ligand binding in hexadecameric rubisco inferred from the crystal structure of the activated unliganded spinach enzyme. *Nature Structural Biology* **3,** 95–101.

Tcherkez GGB, Farquhar GD, Andrews TJ. 2006. Despite slow catalysis and confused substrate specificity, all ribulose bisphosphate carboxylases may be nearly perfectly optimized. *Proceedings of the National Academy of Sciences, USA* **103,** 7246–7251.

Vater J, Salnikow J. 1979. Identification of 2 binding-sites of the D-ribulose-1,5-*bis*phosphate carboxylase-oxygenase from spinach for D-ribulose-1,5-*bis*phosphate and effectors of the carboxylation reaction. *Archives of Biochemistry and Biophysics* **194,** 190–197.

von Caemmerer S. 2000. *Biochemical models of leaf photosynthesis*. Collingwood, Vic: CSIRO Publishing.

von Caemmerer S, Edmondson DL. 1986. Relationship between steady-state gas-exchange, *in vivo* ribulose *bis*phosphate carboxylase activity and some carbon-reduction cycle intermediates in *Raphanus sativus*. *Australian Journal of Plant Physiology* **13,** 669–688.

von Caemmerer S, Farquhar GD. 1985. Kinetics and activation of rubisco and some preliminary modelling of RuP_2 pool sizes. In: Viil J, ed. *Kinetics of photosynthesis*. Tallin, Estonia: Academy of Sciences of the USSR, 46–58.

Ward DA, Keys AJ. 1989. A comparison between the coupled spectrophotometric and uncoupled radiometric assays for RuBP carboxylase. *Photosynthesis Research* **22,** 167–171.

Zhu G, Jensen RG. 1991. Xylulose-1,5-*bis*phosphate synthesized by ribulose-1,5-*bis*phosphate carboxylase/oxygenase during catalysis binds to decarbamylated enzyme. *Plant Physiology* **97,** 1348–1353.